DFT Study of Interaction of Azoles with Cu(111) and Al(111) Surfaces: Role of Azole Nitrogen Atoms and Dipole–Dipole Interactions

Nataša Kovačević and Anton Kokalj*

Department of Physical and Organic Chemistry
Jožef Stefan Institute, Jamova 39, SI-1000 Ljubljana, Slovenia

September 26, 2011

Supporting Information

S1 Lateral Dipole–Dipole Interactions between Polar Adsorbates

For molecules with large dipole moment the lateral dipole–dipole interactions are long ranged and can extent up to several tens of bohrs (e.g., refer to Figure 4 in the manuscript). To better appreciate the significance of these interactions and their dependence on the orientation of molecular dipoles, Figure S1 plots the lateral electrostatic energy as a function of the nearest-neighbor dipole–dipole distance, $R_{\rm nn}$, for several dipole orientations as predicted by the tilted-dipole model, eq (13a) in the manuscript, i.e.,

$$E_{\rm tot}^{\rm dip}(R_{\rm nn}, d_{\rm im}, \mu_0, \alpha, \theta) = -\frac{1}{2}\mu_0^2 \left(\frac{\sin^2\theta}{\xi^{\parallel^{-1}}(R_{\rm nn}, d_{\rm im}) - \alpha} + \frac{\cos^2\theta}{\xi^{\perp^{-1}}(R_{\rm nn}, d_{\rm im}) - \alpha} \right). \quad \text{(S1)}$$

For the definition of the symbols refer to the manuscript. The $d_{\rm im}$, μ_0, and α parameters used in Figure S1 are chosen so as to make the features easily apparent and moreover to be also compatible with the azole molecules. It is clearly seen that lateral interactions are the most important for perpendicularly oriented dipoles, where they are considerably repulsive. The repulsion is reduced with increasing the tilting of dipoles away from the surface normal direction. Lateral interactions finally become attractive for parallel dipoles. An interesting and non-monotonous behavior is displayed by a highly tilted dipoles (blue solid curve): at shorter $R_{\rm nn}$ distances the interactions are attractive ($R_{\rm nn} \lesssim 20$ bohrs) and at larger distances they become repulsive. Such behavior can be attributed to molecular polarizability: at shorter $R_{\rm nn}$ distances it allows the rotation of dipoles toward the parallel direction as to enhance the lateral attraction, whereas at larger $R_{\rm nn}$ distances, where the lateral interactions become small enough, the dipoles are rotated toward the perpendicular direction as to increase the self-interaction of the dipole with its image. Such non-monotonous dependence of lateral interactions as a function of $R_{\rm nn}$ has been also predicted by DFT-GGA calculations for N2-bonded tetrazole on Cu(111) (red curve of Figure 4c in the manuscript).

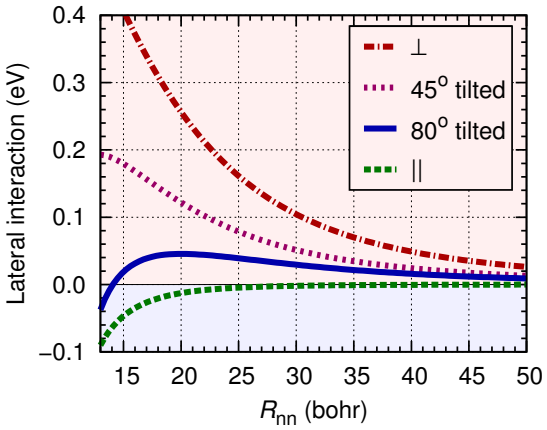

Figure S1. Lateral electrostatic energy, $E_{\rm tot}^{\rm dip}(R_{\rm nn}) - E_{\rm tot}^{\rm dip}(\infty)$, of a hexagonal close-packed layer of polarizable point-dipoles above the metal surface as a function of the nearest neighbor dipole–dipole distance $R_{\rm nn}$ for several dipole orientations. Tilting angle is measured with respect to surface normal, while ⊥ and ∥ symbols stand for dipoles oriented perpendicular and parallel to the surface, respectively. The parameters of the model are the following: μ_0=4 D, α=90 bohr^3, $d_\perp = d_{45^\circ}$=7 bohrs, d_{80°=6 bohrs, and $d_\parallel$=9 bohrs.

S2 Molecular Orbitals of Imidazole, Triazole, Tetrazole, and Pentazole

Figure S2 plots the signed square modulus of frontier molecular orbitals, i.e., $\mathrm{sgn}[\phi(\mathbf{r})] \times |\phi(\mathbf{r})|^2$, of isolated imidazole, triazole, tetrazole, and pentazole molecules. It can be observed that either the HOMO (imidazole) or the LUMO (triazole, tetrazole, and pentazole) is the π-type orbital.

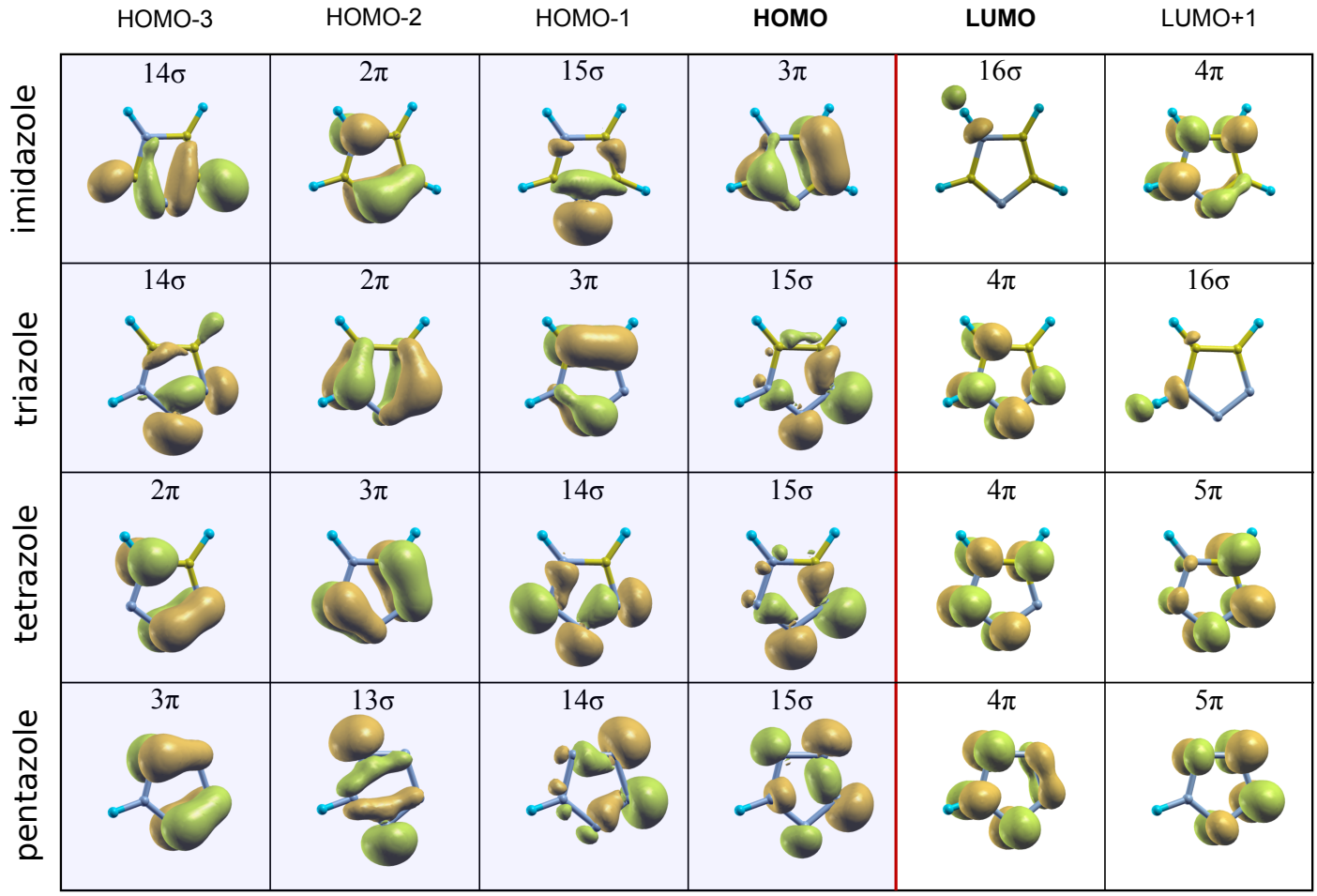

Figure S2. The signed square modulus of molecular orbitals, i.e., $\mathrm{sgn}[\phi(\mathbf{r})] \times |\phi(\mathbf{r})|^2$, of isolated imidazole, triazole, tetrazole, and pentazole molecules. Orbitals from HOMO–3 to LUMO+1 are presented.

S3 Adsorption of Imidazole, Triazole. Tetrazole, and Pentazole on Al(111)

The adsorption of imidazole, triazole, tetrazole, and pentazole on Al(111) has been considered only at 1/25 ML coverage using the (5×5) supercell, which corresponds to the R_{nn} distance of 27.1 bohrs. It can be inferred from the Figure 4 in the manuscript that at this distance the lateral interactions are not sufficient to alter any qualitative trends.

In Table S1 the results of molecular adsorption on Al(111)–(5×5) are compared to those of Cu(111)–(6×6). Note that due to a larger lattice constant of aluminum, the Al(111)–(5×5) supercell corresponds to a hypothetical Cu(111)–(5.5×5.5) supercell, which is why the Cu(111)–(6×6) is presented in the table. It can be observed that on both surfaces the molecule–surface bond strength decreases with increasing the number of nitrogen atoms in azole ring, thus following the order: imidazole > triazole > tetrazole > pentazole. Also the magnitudes of adsorption energies as well as the molecule–metal bond lengths are rather similar on both surfaces for all the molecules. A noteworthy difference between the two surfaces is that on Cu(111) the top and bridge sites are similar in stability, whereas on Al(111) the top sites are more stable.

To provide a further insight into the molecule–surface bonding on Al(111), Figure S3 plots the charge density difference, $\Delta\rho(\mathbf{r}) = \rho_{\mathrm{mol/surf}}(\mathbf{r}) - \rho_{\mathrm{surf}}(\mathbf{r}) - \rho_{\mathrm{mol}}(\mathbf{r})$, and the projected density of states (PDOS) for all the four molecules. The comparison between the Figure S3 and Figure 7 in the manuscript reveals similar patterns of charge redistribution on the molecules for the two surfaces, but the magnitude of molecular charge redistribution appears larger on Al(111). Also the accumulation of charge in the center of the N–Me bond (Me ≡ Al or Cu) as well as the charge redistribution that is characteristic of the N–H$\cdots$Me hydrogen bond are larger on Al(111). Further substantial differences are observed for metal: while on Cu(111) the $\Delta\rho(\mathbf{r})$ pattern resembles the shape of the d_{z^2} orbital, the charge redistribution is far less localized on Al(111), because aluminum is comprised of only delocalized *sp*-states. The 3D isosurface representation of $\Delta\rho(\mathbf{r})$ reveals a blue torus-like electron deficit region on the Al(111) below the molecule (see the inset).

TABLE S1: The PBE calculated adsorption energies and structural parameters of imidazole, triazole, tetrazole, and pentazole adsorbed at 1/25 ML on Al(111) and at 1/36 ML on Cu(111). The former were calculated with the (5×5) and the latter with the (6×6) supercells, which correspond to $R_{\rm nn}$ of 27.1 and 29.5 bohrs, respectively. The corresponding absolute molecular coverages are 5.62×10^{-3} and 4.75×10^{-3} molecule/Å^2 on Al(111) and Cu(111), respectively.

Surface	Molecule	Adsorption mode	$E_{\rm ads}$ (eV)	$d_{\rm N2-Al}$ (Å)	$d_{\rm N3-Al}$ (Å)	$d_{\rm N4-Al}$ (Å)
Al(111)–(5×5)						
	imidazole	N3	−0.65	/	2.09	/
	triazole	N2	−0.45	2.13	/	/
		N2+N3	−0.29	2.14	2.16	/
		N3	−0.43	/	2.15	/
	tetrazole	N2	−0.30	2.20	/	/
		N3+N4	−0.17	/	2.17	2.19
		N4	−0.35	/	/	2.16
	pentazole	N2	−0.13	2.21	/	/
		N3+N4	0.00	/	2.24	2.26

Surface	Molecule	Adsorption mode	$E_{\rm ads}$ (eV)	$d_{\rm N2-Cu}$ (Å)	$d_{\rm N3-Cu}$ (Å)	$d_{\rm N4-Cu}$ (Å)
Cu(111)–(6×6)						
	imidazole	N3	−0.63	/	2.09	/
	triazole	N2	−0.47	2.11	/	/
		N2+N3	−0.46	2.15	2.16	/
		N3	−0.45	/	2.11	/
	tetrazole	N2	−0.34	2.13	/	/
		N3+N4	−0.35	/	2.19	2.14
		N4	−0.39	/	/	2.12
	pentazole	N2	−0.21	2.16	/	/
		N3+N4	−0.11	/	2.20	2.16

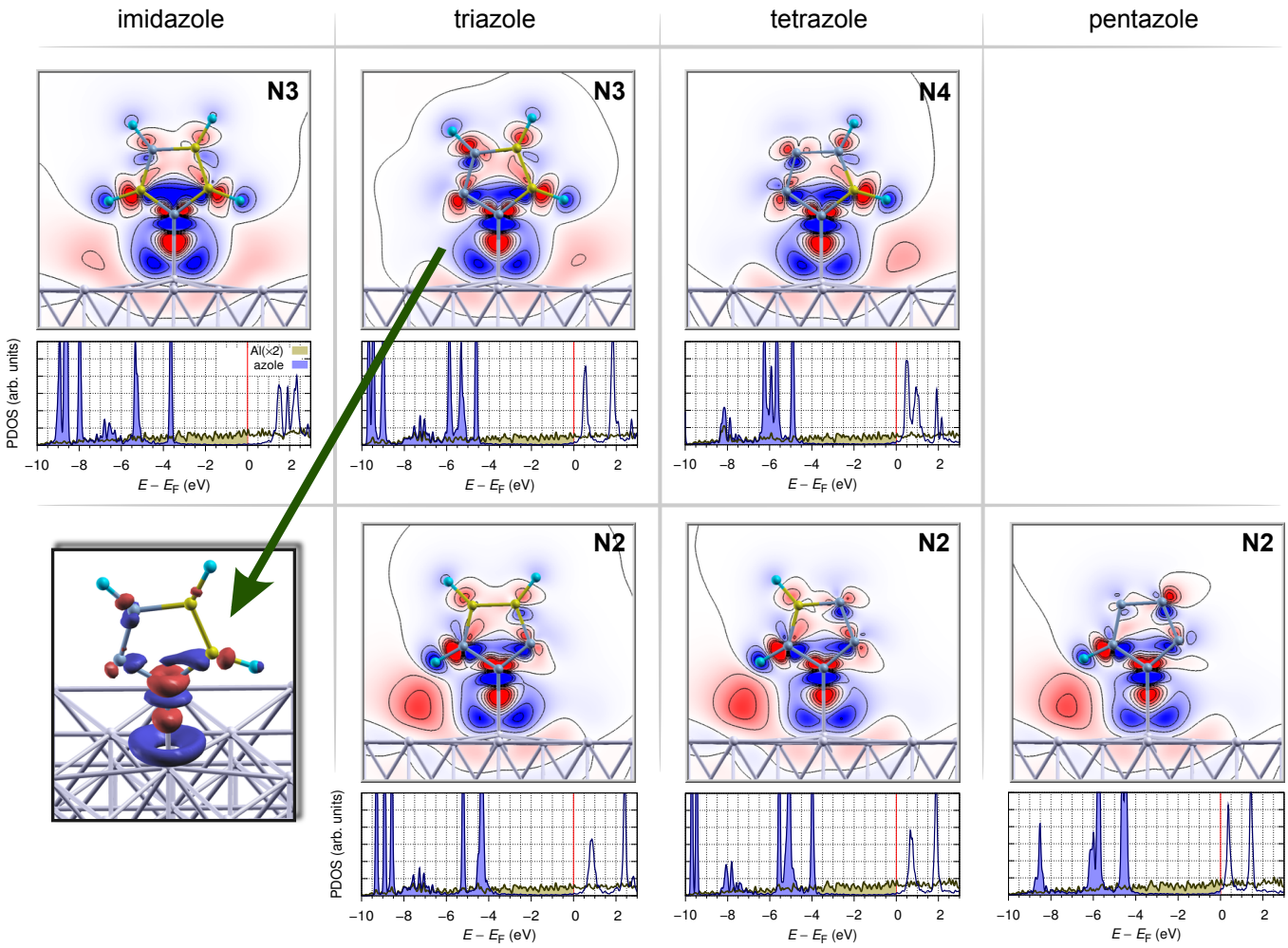

Figure S3. Charge density difference, $\Delta\rho(\mathbf{r}) = \rho_{\rm mol/surf}(\mathbf{r}) - \rho_{\rm surf}(\mathbf{r}) - \rho_{\rm mol}(\mathbf{r})$, and density of states projected to the molecule (blue) and the Al atom (olive-green) beneath it for the four considered molecules on Al(111). The $\Delta\rho(\mathbf{r})$ plots are drawn with seven contours in linear scale from −0.006 to +0.006 e/a_0^3; the blue (red) color represents the electron deficit (excess) regions, i.e., charge flows from blue to red regions. Inset shows the 3D isosurface representation of $\Delta\rho(\mathbf{r})$ of N3-adsorbed triazole with isosurfaces drawn at ±0.005 e/a_0^3.